University Library

MINERVA ACCESS

A gateway to Melbourne's research publications

Minerva Access is the Institutional Repository of The University of Melbourne

Author/s:
Gray, HA;Guan, S;Thomeer, LT;Schache, AG;de Steiger, R;Pandy, MG

Title:
Three-dimensional motion of the knee-joint complex during normal walking revealed by mobile biplane x-ray imaging

Date:
2019-03-01

Citation:
Gray, H. A., Guan, S., Thomeer, L. T., Schache, A. G., de Steiger, R. & Pandy, M. G. (2019). Three-dimensional motion of the knee-joint complex during normal walking revealed by mobile biplane x-ray imaging. Journal of Orthopaedic Research, 37 (3), pp.615-630. https://doi.org/10.1002/jor.24226.

Persistent Link:
https://hdl.handle.net/11343/285494

Research Article (Member)

Three-dimensional Motion of the Knee-joint Complex during Normal Walking Revealed by Mobile Biplane X-ray Imaging[1]

Hans A. Gray 0000-0002-2587-8747 0000-0002-2587-8747[1], Shanyuanye Guan[1], Lucas T. Thomeer[1], Anthony G. Schache[1], Richard de Steiger[2], Marcus G. Pandy[1]

[1]Department of Mechanical Engineering, University of Melbourne, Victoria 3010, Australi 0000-0002-5704-9644a

[2]Department of Surgery, Epworth Health Care, University of Melbourne, Victoria 3010, Australia

Submitted as a Research Article to the *Journal of Orthopaedic Research*

Word count (Introduction through Discussion): 4686

11 December 2018

Corresponding Author:

Author Manuscript

[1] This is the author manuscript accepted for publication and has undergone full peer review but has not been through the copyediting, typesetting, pagination and proofreading process, which may lead to differences between this version and the Version of Record. Please cite this article as doi:10.1002/jor.24226

This article is protected by copyright. All rights reserved.

Marcus G. Pandy, Ph.D.
Department of Mechanical Engineering
The University of Melbourne
Parkville, Victoria 3010, Australia
Email: pandym@unimelb.edu.au, phone: +61 3 8344 4054, fax: +61 3 9347 8784

Running title: Knee-joint Motion in Human Gait

Author Contributions

HAG, SG, AGS, RdeS and MGP designed the study. MGP and RdeS obtained funding for the research. HAG, SG and LTT performed the data collection and analysis. HAG, SG and MGP interpreted the data and drafted the manuscript. All authors edited, revised and approved the final version. MGP was the chief investigator for the study.

Author Manuscript

Abstract

Accurate knowledge of knee kinematics is important for a better understanding of normal joint function and for improving patient outcomes subsequent to joint reconstructive surgery. Limited information is available that accurately describes the relative movements of the bones at the knee in vivo, even for the most common of all activities: walking. We used a mobile X-ray imaging system to measure the three-dimensional motion of the entire knee-joint complex – femur, tibia and patella – when humans walk over ground at their natural speeds. Data were recorded from 15 healthy individuals (9 males, 6 females; age 30.5±6.2 years). The most pronounced rotational motion of the tibia was flexion-extension followed by internal-external rotation and abduction-adduction (peak-to-peak displacements: 70.7°, 9.2° and 1.9°, respectively). Maximum anterior translation of the tibia was 6.5 mm and occurred in early swing, coinciding with peak knee flexion and peak internal rotation. The most prominent rotational motion of the patella was flexion-extension (peak-to-peak displacement: 50.5°). The tibia pivoted about the medial compartment of the tibiofemoral joint, conferring greater movements of the contact centers in the lateral compartment than the medial compartment (15.4 mm and 9.7 mm, respectively). Internal-external rotation, anterior-posterior translation and medial-lateral shift of the tibia as well as flexion-extension and anterior-posterior translation of the patella were each coupled to the knee flexion angle, as were movements of the contact centers at each joint. These fundamental data serve as a valuable resource for evaluating knee joint function in normal and pathological gait. The data are available in Supplementary_Material_Data.xlsx.

Keywords

Patellofemoral, tibiofemoral, standing, joint coupling, knee model

Author Manuscript

Introduction

The knee is a complex system consisting of three bones and two joints: the femur and tibia articulate at the tibiofemoral joint; and the femur and patella, at the patellofemoral joint. Both joints must withstand high contact forces (well in excess of body weight) during daily activities such as walking[1]. Accurate knowledge of three-dimensional knee kinematics and condylar motion is important for a better understanding of normal and pathological joint function, and ultimately for improving patient outcomes subsequent to total knee arthroplasty, knee-ligament reconstruction and high tibial osteotomy. Knee-joint biomechanics has been studied for well over a century, yet only two studies have recorded the full three-dimensional movements of the femur and tibia for one complete cycle of normal walking (i.e., heel-strike to the next ipsilateral heel-strike)[2,3], and no data to our knowledge are available to describe the corresponding motion of the patella.

The most common method for measuring joint motion in vivo involves video-based motion capture with reflective markers fixed on the skin. Unfortunately, movement of the skin with respect to bone causes uncertainty in the measured joint kinematics, with root-mean-square (RMS) errors as high as 24 degrees reported for bone motion at the knee[4]. Errors due to skin movement may be minimized, if not eradicated, by inserting steel pins directly into bone[2,5,6]; however, intra-cortical pins cause pain and impingement, potentially altering the subject's natural gait pattern[7].

Dynamic X-ray imaging (or fluoroscopy) enables accurate, non-invasive measurement of bone motion in vivo. Single and biplane X-ray imaging have been used to measure motion of the

Author Manuscript

healthy knee during both walking and running gaits[8–11]. In these studies, the imaging equipment remained fixed relative to the ground while subjects ambulated on a treadmill. Thus, even for relatively slow walking speeds, it has been possible to analyze only a portion of the stride cycle because the joint invariably strays beyond the capture volume of the X-ray imaging device[8–12].

X-ray fluoroscopy also has been used to measure the locations of the tibiofemoral joint contact centers during weight-bearing activities such as lunging[13,14]. The results indicate that the contact center moves further in the lateral compartment than in the medial compartment, suggesting that the femur pivots about the medial tibial condyle and that axial rotation of the tibia is coupled to the knee flexion angle[15]. Indeed, the results of cadaver experiments suggest that the healthy knee has two primary axes of rotation fixed in bone: an optimal flexion axis that passes through the centers of the femoral condyles, and a longitudinal axis that is parallel to the mechanical axis of the tibia and passes through the medial joint compartment[16,17]. These findings have driven recent innovations in total knee replacement design such as the development of a medially-constrained knee implant[18], where the medial tibiofemoral articulation is fashioned as a ball-and-socket joint to restrict anterior-posterior movement of the medial femoral condyle. The hypothesis that the healthy knee pivots about the medial tibiofemoral compartment was recently challenged by Koo and Andriacchi[19] who, using skin-surface markers, found the center of rotation in the transverse plane to lie in the lateral compartment during the stance phase of walking.

Here we provide the first non-invasive measurements of the kinematics of the entire knee-joint complex for normal walking. We used a unique Mobile Biplane X-ray (MoBiX) imaging system[20] to track and image the three-dimensional motion of the femur, tibia and patella as

Author Manuscript

healthy young adults walked at their natural speeds over ground. Our specific aims were to (1) obtain simultaneous measurements of 6-degree-of-freedom (6-DOF) tibiofemoral and patellofemoral joint kinematics and condylar motion for one complete stride cycle; (2) examine the extent to which secondary rotations and translations of the femur, tibia and patella are coupled to the knee flexion angle; and (3) determine the location of the center of rotation of the knee in the transverse plane for the stance and swing phases of normal walking.

Materials and Methods

Design: Descriptive cross-sectional study

Level of Evidence: III

Participants

Fifteen healthy individuals (9 males and 6 females; age 30.5 ± 6.2 years; height, 168.0 ± 9.3 cm; weight, 67.4 ± 8.4 kg) with no knee pain and no history of knee surgery gave informed consent to participate in this study. Ethics approval for the experimental procedures was granted by the Human Research Ethics Committee at the University of Melbourne.

Experimental protocol

Biplane X-ray images (resolution 1024×1024 pixels) of the right knee were acquired using the MoBiX imaging system (Fig. 1A) sampling at 200 frames/sec with an exposure time of 1/200 sec. Design specifications and performance of the MoBiX imaging system are described in detail by Guan et al.[20]. The X-ray units were operated in continuous mode (110 kV and 13.1 mA) with an inter-beam angle of approximately 60° and an X-ray source to image intensifier distance of

Author Manuscript

approximately 1.4 m. Body-segmental motion and ground reaction forces were recorded synchronously with the X-ray images. Full-body 3D motion data were recorded using a 9-camera video-based motion capture system (VICON, Oxford, UK) sampling at 120 Hz, while ground reaction forces were measured using three strain-gauged force plates (AMTI, Watertown, MA) sampling at 1080 Hz and mounted flush with an 8.4 m long wooden walkway. In addition, a CT scan (voxel size 0.35x0.35x0.50 mm) of the right knee was obtained with the joint extended. Each participant was exposed to a maximum combined radiation dosage of 0.18 mSv from both biplane X-ray imaging and the CT scan.

All participants completed two sessions. The first session involved a 1-hour familiarization procedure that gave each participant the opportunity to practice walking with the MoBiX system operational. The second session involved gait data collection. Each participant wore a sleeveless top, lead vest, shorts and sandals. Forty-five retro-reflective skin markers were placed at predetermined landmarks[21]. The participant walked back and forth in a straight line several times at a comfortable speed while average stride length was measured and used to mark the locations of the first 3 steps on the walkway (R1, L1 and R2 in Fig. 1B). Each trial consisted of 10 complete steps, with foot placement prescribed only for the first 3 steps; the subject was free to choose foot placement, and hence step length, for the remaining 7 steps of each trial. This protocol was adopted to ensure the participant used a comfortable step length and stepped onto the three force plates during the 4^{th}, 5^{th} and 6^{th} steps (L2, R3, L3, respectively, in Fig. 1B). The MoBiX system tracked and imaged the right knee of the participant during the mid-portion of the walking trial, from the 2^{nd} right-heel-strike to the 4^{th} right-heel-strike (i.e., two complete stride cycles from R2 to R4 in Fig. 1B). Kinematic data were processed for one complete stride cycle,

Author Manuscript

from the 3rd right heel-strike to the 4th right heel-strike (R3 to R4 in Fig. 1B). Kinematic and kinetic data were also recorded for a static trial in which the subject stood on one force plate with the arms abducted away from the trunk and the feet set apart at approximately shoulder width.

Knee-joint kinematics

6-DOF tibiofemoral and patellofemoral joint kinematics were derived from the biplane X-ray images by following a pipeline of previously described procedures[20]. Image processing, pose estimation, and joint kinematic analysis were performed using a custom program developed in MATLAB (Mathworks Inc., Natick, MA). Maximum RMS errors associated with 6-DOF kinematic measurements for the healthy knee during overground walking were reported to be 0.78 mm and 0.77° for translations and rotations of the tibiofemoral joint[20] and 0.37 mm and 1.46° for translations and rotations of the patellofemoral joint[22]. Individual geometric models of the femur, tibia and patella, required for pose estimation, were segmented from the CT images using 3D Slicer[23]. An anatomical joint coordinate system[24] was developed to describe 6-DOF kinematics of both the tibiofemoral and patellofemoral joints (see Fig. 2). Raw kinematic measurements were filtered using a fourth-order, low-pass Butterworth filter with a cut-off frequency of 10 Hz and then resampled to 201 time points over one stride cycle. Major gait events were identified using the full-body motion data and ground force measurements[25].

Condylar motion and knee-joint center of rotation

Femoral condylar motion was determined by identifying the approximate geometric center of each femoral condyle and calculating its position with respect to the tibia at each time point during the stride cycle. The centers of the femoral condyles were found by determining the

Author Manuscript

intersection between the medial-lateral axis of the femur (axis X_F in Fig. 2) and the approximate mid-sagittal plane of each condyle.

The kinematic measurements and shapes of the articulating surfaces of the bones were used to estimate the locations of joint contact between the femur and tibia and between the femur and patella. The contact centers in the medial and lateral compartments of the tibiofemoral joint were found by identifying the minimum distances between the medial and lateral condyles of the femur and a transverse plane fitted to the tibial plateau[26]. The contact centers for the patellofemoral joint were found by calculating the locations of points on the medial and lateral patellar facets that were closest to the femoral surface.

The center of rotation of the knee in the transverse plane was found by projecting the medial-lateral axis of the femur (axis X_F in Fig. 2) onto the transverse plane of the tibia ($X_TO_TY_T$ plane in Fig. 2) at each time point, and the intersection of these projections was then calculated on a least-squares basis[19] for the stance phase, swing phase, and the entire stride cycle.

Normalization

Joint translations, locations of the femoral condylar centers, locations of joint contact, and the center of rotation of the knee in the transverse plane were each normalized on a participant-specific basis using a coefficient (C_i) defined as follows:

$$C_i = \frac{\bar{w}}{w_i}$$

Author Manuscript

where w_i is the femoral bicondylar width measured for the i[th] participant and $\bar{w}$ is the mean femoral bicondylar width calculated across all participants[27].

Statistical analyses

Means and standard deviations were calculated for tibiofemoral and patellofemoral joint kinematics, motion of the femoral condylar centers and tibiofemoral joint contact centers, and the center of rotation of the knee in the transverse plane. Student's paired t-tests were used to compare (1) peak values of 6-DOF knee-joint kinematics and the displacements of the condylar centers and joint contact centers measured for walking against mean values of the corresponding variables measured for standing; (2) peak-to-peak displacements of the condylar centers on the medial and lateral sides of the knee; and (3) peak-to-peak displacements of the joint contact centers in the medial and lateral compartments of the knee. Two-sided, two-sample t-tests were used to compare parameters between males and females. Differences were considered statistically significant when $p<0.05$.

We used a curve-fitting technique to assess the degree to which secondary motions of the tibia and patella relative to the femur were coupled to the knee flexion angle. For example, coupling between lateral shift of the tibia and the knee flexion angle was evaluated by fitting a spline function to the 201 data points in the graph of mean lateral tibial shift versus mean knee flexion; the spline was generated using a MATLAB function called 'fit' (Mathworks Inc., Natick, MA), which applied a least-squares approximation with the 'smoothing parameter' set to 0.1. The coefficient of determination (r^2) and the Root Mean Square Error (RMSE) associated with this fit were used as indicators of how strongly lateral tibial shift was coupled to the knee flexion angle.

Author Manuscript

An r^2 value of 1.0 and RMSE of 0.0 would indicate perfect coupling between the two variables. Details of these methods are provided in Supplementary_Material_Methods.docx.

Results

Mean walking speed across all participants was 1.28 ± 0.15 m/s (range: 1.03 to 1.51 m/s). No statistically significant differences were found in either tibiofemoral or patellofemoral joint kinematics measured for the male and female participants, thus all data were pooled.

Tibiofemoral kinematics

The most pronounced rotational motion of the tibia was flexion-extension (peak-to-peak displacement, 70.7°). The magnitudes of internal-external rotation (peak-to-peak displacement, 9.2°) and abduction-adduction (peak-to-peak displacement, 1.9°) were much smaller, the latter deviating relatively little throughout the stride cycle (Fig. 3A, Table 1). The largest translational motion of the tibia was anterior-posterior translation (peak-to-peak displacement, 6.4 mm) followed by medial-lateral shift (peak-to-peak displacement, 4.0 mm) and compression-distraction (peak-to-peak displacement, 1.0 mm).

The knee was slightly bent at heel-strike and proceeded to flex during early stance to a maximum of 14.1° at contralateral toe-off (Fig. 3A). It then extended to a minimum flexion angle of 1.0° just prior to contralateral heel-strike. Terminal stance was marked by rapid flexion, which continued into swing until the flexion angle reached a maximum of 68.6° immediately after toe-off. The knee then extended for most of the swing phase and became hyperextended just before heel-strike. The tibia was internally rotated for most of the walking cycle (Fig. 3A). Maximum

internal rotation (external rotation angle of -5.4°) occurred during swing and coincided with peak knee flexion immediately after toe-off. As the knee extended through swing the tibia rotated externally to its maximum value of 3.8° just before heel-strike.

The tibia translated anteriorly from heel-strike and reached a peak position of 3.7 mm at contralateral toe-off (Fig. 3A). Maximum anterior translation (6.5 mm) occurred in early swing, coinciding with peak knee flexion and peak internal rotation (Fig. 3A). The tibia then translated posteriorly with knee extension. Medial-lateral translation of the tibia was minimal during the first half of the stride cycle (Fig. 3A). During late stance and early swing, the tibia translated medially and then laterally, reaching a peak position of 2.3 mm just before heel-strike. Compression-distraction and abduction-adduction were small with nondescript profiles that appeared to be unrelated to the flexion angle (Fig. 3A and B, Table 1).

Internal-external rotation, anterior-posterior translation and medial-lateral shift were each coupled to the knee flexion angle ($r^2 > 0.76$ for all) (Fig. 3B). An increase in knee flexion was associated with internal rotation, anterior translation and medial shift of the tibia relative to the femur.

Author Manuscript

Patellofemoral kinematics

The most prominent rotational motion of the patella was flexion-extension (peak-to-peak displacement, 50.5°); medial-lateral tilt and medial-lateral rotation were relatively small (peak-to-peak displacements of 4.5° and 3.8°, respectively) and displayed unremarkable profiles (Fig. 4A, Table 1). The largest translational motion was superior-inferior translation (peak-to-peak

displacement, 14.9 mm) followed by anterior-posterior translation (peak-to-peak displacement, 11.3 mm) and medial-lateral shift (peak-to-peak displacement, 4.9 mm).

The time course of patellar flexion was closely similar to that of knee flexion (cf Figs 3A and 4A). Patellar flexion exhibited two maxima, each coinciding with a peak in the knee flexion angle. The patella flexed through weight acceptance and attained a peak of 10.0° shortly after contralateral toe-off. It then flexed rapidly in late stance and early swing, reaching a peak of 47.4° immediately after toe-off.

The patella underwent rapid superior translation just after heel-strike and continued to translate superiorly during mid-stance, reaching a peak superior position of 17.2 mm (Fig. 4A and B). It then translated inferiorly in late stance before reaching its most inferior position of 2.3 mm shortly after toe-off, when both knee flexion and patellar flexion were maximum. The patella translated superiorly and inferiorly by relatively small amounts (~ 4 mm) during swing before translating rapidly in the superior direction immediately before heel-strike. Peak-to-peak displacements for patellar rotation, tilt and shift were comparable during stance and swing: the patella rotated, tilted and shifted by 3.8°, 4.5°, and 4.0 mm, respectively, during stance compared to corresponding movements of 2.5°, 3.1°, and 3.6 mm in swing.

Patellar flexion was tightly coupled ($r^2 = 0.998$) and linearly related (coefficient of determination for linear regression = 0.99) to the knee flexion angle (Fig. 4B). Patellar flexion lagged knee flexion for nearly the entire stride cycle, especially during swing when the knee was highly flexed. Anterior-posterior translation of the patella also was tightly coupled ($r^2 = 0.97$) and

Author Manuscript

linearly related (coefficient of determination for linear regression = 0.94) to the knee flexion angle, with an increase in knee flexion associated with posterior translation of the patella (Fig. 4A and B). Medial-lateral tilt and medial-lateral shift were coupled to knee flexion when the knee was bent beyond 20°.

Condylar motion and joint center of rotation in the transverse plane

The centers of the medial and lateral femoral condyles translated predominantly in the anterior-posterior direction during walking (Fig. 5, Table 2). Both condyles translated posteriorly as the knee flexed during late stance and early swing, with peak-to-peak displacement of the lateral condyle (11.6 mm) being significantly greater than that of the medial condyle (7.6 mm, $p<0.001$). Peak-to-peak displacements of the two condyles in the medial-lateral direction were similar throughout one stride.

Consistent with the movements of the centers of the femoral condyles, anterior-posterior translation of the tibiofemoral contact center was greater in the lateral compartment than the medial compartment (Fig. 6A and B). Mean anterior-posterior displacement of the contact center in the lateral compartment was 15.4 mm compared to 9.7 mm in the medial compartment ($p = 0.002$, Table 2). Movements of the contact centers in the medial and lateral compartments were coupled to the knee flexion angle ($r^2 > 0.85$), with posterior translations of the contact centers on the medial and lateral tibial plateaux associated with increasing knee flexion (Fig. 6C).

In contrast, the patterns of movement of the contact centers on the medial and lateral facets of the patella were similar (Fig. 7A and B). Both contact centers remained on the inferior half of the

patella for most of the stance phase, before translating first superiorly and then inferiorly during swing. Superior-inferior translations of the patellar contact centers were larger than those observed in the medial-lateral direction ($p<0.02$, Table 2), and were coupled to the knee flexion angle ($r^2 > 0.92$). Superior translations of the contact centers on the medial and lateral facets of the patella were related to increases in knee flexion (Fig. 7C).

The center of rotation of the tibiofemoral joint in the transverse plane was located at an average distance of 17.9 mm medial to the tibial origin over one stride cycle (Fig. 8). During stance the center of rotation was close to the geometric center of the tibial plateau and positioned 5.8 mm medially, whereas in swing it shifted further medially to be located 36.1 mm medial to the tibial origin.

Knee-joint configuration in standing

The knee was more hyperextended and the tibia more externally rotated in standing than at any time during walking. Knee hyperextension in standing was 5.8° compared to a maximum hyperextension of 3.2° attained in walking ($p = 0.02$). The tibia was externally rotated by 8.1° in standing whereas maximum external rotation during walking was 5.0° ($p = 0.002$, Table 2). The tibiofemoral contact center was translated more anteriorly in the lateral compartment (9.3 mm) than in the medial compartment (3.1 mm) during standing ($p = 0.004$) (Fig. 6A and B; Table 2). Anterior translation of the lateral contact center was also greater during standing (9.3 mm) than at any time during walking (6.1 mm peak displacement, $p = 0.04$). The patella was displaced more laterally and anteriorly in standing compared to walking; however, patellar tilt was not significantly different (Fig. 4A, Table 2).

Author Manuscript

Discussion

We used a unique mobile biplane X-ray imaging system to obtain simultaneous measurements of 6-DOF kinematics of the healthy tibiofemoral and patellofemoral joints for one complete stride cycle when humans walk over ground at their natural speeds. We found that internal-external rotation, anterior-posterior translation and medial-lateral shift of the tibia as well as flexion-extension, anterior-posterior translation and, to a lesser extent, medial-lateral tilt and medial-lateral shift of the patella are each coupled to the knee flexion angle. Anterior-posterior translations of the tibiofemoral contact centers were significantly greater in the lateral compartment than the medial compartment whereas no appreciable differences were observed in the movements of the contact centers on the medial and lateral facets of the patella. Posterior translations of the tibiofemoral contact centers and superior translations of the patellofemoral contact centers were associated with increasing knee flexion. The center of rotation of the knee in the transverse plane was located predominantly on the medial side throughout one stride cycle. These fundamental data provide an accurate description of the kinematic behavior of the entire knee-joint complex during normal walking and serve as a valuable resource for evaluating tibiofemoral and patellofemoral function in pathological gait. Accurate knowledge of 6-DOF knee kinematics is also essential for validating computational models of the knee joint. Measured 6-DOF rotations and translations of the tibia and patella relative to the femur are available in Supplementary_Material_Data.xlsx.

One potential limitation of the present study relates to the use of a mobile gantry mechanism, which, by translating the imaging units alongside the participants, may have adversely affected their natural gait. To address this concern, we provided ample opportunity for each participant to

Author Manuscript

practice walking with the MoBiX system in operation, first during an initial familiarization session and subsequently on the day of testing immediately prior to data collection. Yamokoski and Banks[28] quantified the errors associated with the measurement of free-speed gait kinematics when humans are followed by a mobile imaging system. They found that a close-proximity robot motion tracking system increased stride length by just 9 mm and resulted in no statistically significant differences in hip- and knee-joint motion compared to normal gait. A second limitation is that the locations of the joint contact centers were calculated using the surface geometries of the bones reconstructed from a CT scan of each participant's knee. More accurate assessment of the joint contact center locations, particularly near full extension of the knee, may be derived using geometric models of the bones, cartilage and menisci obtained from MRI.[29] In addition, the locations of the joint contact centers at the patellofemoral joint were calculated by assuming that contact occurred on both facets of the patella. While this is likely to be the case for most of the stride cycle when the patella is firmly entrenched in the trochlear groove, contact between the articular surfaces of the patella and femur may not be guaranteed when the knee is near full extension.

The only comparable datasets describing knee kinematics in healthy overground gait are those of LaFortune et al.[2] and Andriacchi et al.[3] who used bone pins and skin markers, respectively, to measure 6-DOF tibiofemoral joint kinematics during overground walking. Our results for flexion-extension, internal-external rotation and medial-lateral shift are consistent with the corresponding patterns of movement noted by LaFortune et al.[2], but there is less agreement in the remaining three degrees of freedom of tibiofemoral joint motion (Fig. 9). The amplitude of anterior-posterior translation measured in the present study is smaller and displays a noticeably

Author Manuscript

different profile for most of the stride cycle. Our measurements of joint compression-distraction are also larger than those of LaFortune, especially during late stance and the first half of swing. These authors assigned 3D coordinate systems to the femur and tibia based on bony landmarks identified from 2D X-ray images whereas we used more accurate 3D models segmented from CT scans. Intracortical pins also cause pain and impingement, which may have altered the gait patterns of the participants in LaFortune's study, plus this technique is prone to errors caused by vibration, bending and loosening of the bone pins[7]. There are notable differences also between our measurements and those of Andriacchi et al.[3], particularly with respect to internal-external rotation, abduction-adduction, anterior-posterior translation and medial-lateral shift (Fig. 9).

Coupled motions have been studied in the unloaded knee by measuring unconstrained passive kinematics in cadaver specimens[30]. Internal rotation, adduction and all three components of tibial translation were found to be coupled to the flexion angle in both passive flexion and extension, implying that the knee behaves as a 1-DOF mechanism with the relative movements of the bones guided solely by ligament geometry and articular contact. Our data show that internal-external rotation, anterior-posterior translation and medial-lateral shift of the tibia are each coupled to knee flexion-extension during walking, but no clear association was observed between the flexion angle and abduction-adduction (Fig. 3B). We also found that movements of the tibiofemoral contact centers in both the medial and lateral compartments are coupled to the knee flexion angle, with posterior translations of the contact centers (i.e., rollback of the medial and lateral femoral condyles on the tibial plateau) associated with increasing knee flexion (Fig. 6C). These results are consistent with the hypothesis that the knee may be approximated as a 1-DOF mechanical linkage and suggest that, at least for normal walking, tibial internal-external rotation,

Author Manuscript

anterior-posterior translation and medial-lateral shift depend more heavily upon the soft-tissue structures and bony anatomy of the knee than the external (muscle, gravitational and inertial) forces transmitted at the joint.

Previous investigators have shown that the tibia rotates internally as the knee is flexed, and that this rotation is reversed in the classic 'screw-home' pattern during extension[31]. In the present study, knee extension was associated with external rotation of the tibia, which was particularly evident as the knee approached full extension (Fig. 3B). Indeed, the tibia was externally rotated by as much as 8° while the knee was hyperextended in standing (Fig. 3B), with the tibiofemoral contact center translated 6 mm more anteriorly in the lateral compartment than the medial compartment (green diamonds in Fig. 6A). These results illustrate clearly the existence of a screw-home pattern of movement in the healthy joint.

The tibia was more anteriorly translated at contralateral toe-off compared to its configuration at the same flexion angle during swing (Fig. 2B). Movement of the tibia during early stance, and particularly near contralateral toe-off, may be explained by the action of the quadriceps muscles, which are shown to be active at this time[32]. During early stance, when the knee is near extension, the line-of-action of the patellar tendon is such that it applies an anterior shear force to the tibia[33] Thus, any force transmitted from the quadriceps to the patellar tendon will act to translate the tibia anteriorly at this time.

The quadriceps likely played a major role in stabilizing motion of the patella during terminal swing as the knee approached hyperextension (Fig. 4B). During the latter half of swing the

Author Manuscript

patella descended inferiorly and the patellar tendon was then presumably slack. Activation of the quadriceps muscles prior to heel-strike[34] translated the patella rapidly in the superior direction, allowing the patellar tendon to become taut once more. As the knee flexed beyond 20°, anterior-posterior translation, medial-lateral tilt and medial-lateral shift of the patella were each tightly coupled with the knee flexion angle (Fig. 4B), indicating that the patella was then firmly entrenched within the trochlear groove.

Our measurements suggest that the center of rotation of the knee in the transverse plane lies in the medial compartment of the tibiofemoral joint during both stance and swing. Using video motion capture with skin markers, Koo and Andriacchi[19] found that the center of rotation was located in the lateral compartment during stance. This discrepancy may be due to the different measurement methods adopted in these two studies. Using biplane X-ray imaging, Liu et al.[35] also found the center of rotation in the transverse plane to lie in the lateral compartment during stance. However, the subjects in their study walked on a treadmill at the relatively slow speed of 0.67 m/s. Guan et al.[25] found statistically significant differences between treadmill and overground walking with respect to 6-DOF tibiofemoral kinematics and the locations of the joint contact centers when subjects walked at the same speed under these two conditions. In addition, the walking speed of 0.67 m/s reported by Liu et al. (2010) is approximately one-half of the preferred speed adopted by the subjects in the present study (1.28 m/s). Our findings concur with previous reports which show that the longitudinal axis of rotation passes through the medial tibial plateau, indicating that axial rotation of the knee occurs about the medial compartment of the tibiofemoral joint[15–17]. Our results also show that anterior-posterior translation of the center of the lateral femoral condyle is significantly greater than that of the medial femoral condyle

Author Manuscript

(Fig. 5A and B), consistent with the concept of a medially-constrained total knee replacement design[18].

Acknowledgments

This work was supported in part by funding from the Australian Research Council Discovery Projects Scheme, Grant DP120101973, and the Victorian Orthopaedic Research Trust.

Conflict of interests

The authors declare no conflict of interests.

Author Manuscript

References

1. Pandy MG, Andriacchi TP. 2010. Muscle and joint function in human locomotion. Annu Rev Biomed Eng 12:401–433.

2. LaFortune MA, Cavanagh PR, Sommer HJ, Kalenak A. 1992. Three-dimensional kinematics of the human knee during walking. J Biomech 25:347–357.

3. Andriacchi TP, Alexander EJ, Toney MKK, et al. 1998. A point cluster method for in vivo motion analysis: applied to a study of knee kinematics. J Biomech Eng 120:743–749.

4. Akbarshahi M, Schache AG, Fernandez JW, et al. 2010. Non-invasive assessment of soft-tissue artifact and its effect on knee joint kinematics during functional activity. J Biomech 43:1292–301.

5. Reinschmidt C, Van Den Bogert AJ, Lundberg A, et al. 1997. Tibiofemoral and

tibiocalcaneal motion during walking: External vs. skeletal markers. Gait Posture 6:98–109.

6. Benoit DL, Ramsey DK, Lamontagne M, et al. 2007. In vivo knee kinematics during gait reveals new rotation profiles and smaller translations. Clin Orthop Relat Res 454:81–88.

7. Ramsey DK, Wretenberg PF, Benoit DL, et al. 2003. Methodological concerns using intra-cortical pins to measure tibiofemoral kinematics. Knee Surgery, Sport Traumatol Arthrosc 11:344–349.

8. Kozanek M, Hosseini A, Liu F, et al. 2009. Tibiofemoral kinematics and condylar motion during the stance phase of gait. J Biomech 42:1877–1884.

9. Anderst W, Zauel R, Bishop J, et al. 2009. Validation of three-dimensional model-based tibio-femoral tracking during running. Med Eng Phys 31:10–16.

10. Farrokhi S, Voycheck CA, Klatt BA, et al. 2014. Altered tibiofemoral joint contact mechanics and kinematics in patients with knee osteoarthritis and episodic complaints of joint instability. Clin Biomech 29:629–635.

11. Kefala V, Cyr AJ, Harris MD, et al. 2017. Assessment of knee kinematics in older adults using high-speed stereo radiography. Med Sci Sports Exerc 49:2260–2267.

12. Li C, Hosseini A, Tsai T-Y, et al. 2015. Articular contact kinematics of the knee before and after a cruciate retaining total knee arthroplasty. J Orthop Res 33:349–358.

13. Komistek RD, Dennis DA, Mahfouz M. 2003. In vivo fluoroscopic analysis of the normal human knee. Clin Orthop Relat Res 410:69–81.

14. Li G, DeFrate LE, Sang EP, et al. 2005. In vivo articular cartilage contact kinematics of

Author Manuscript

the knee: An investigation using dual-orthogonal fluoroscopy and magnetic resonance image-based computer models. Am J Sports Med 33:102–107.

15. Freeman MAR, Pinskerova V. 2005. The movement of the normal tibio-femoral joint. J Biomech 38:197–208.

16. Hollister AM, Jatana S, Singh AK, et al. 1993. The axes of rotation of the knee. Clin Orthop Relat Res 290:259–268.

17. Churchill DL, Incavo SJ, Johnson CC, Beynnon BD. 1998. The transepicondylar axis approximates the optimal flexion axis of the knee. Clin Orthop Relat Res 356:111–118.

18. Scott G, Imam MA, Eifert A, et al. 2016. Can a total knee arthroplasty be both rotationally unconstrained and anteroposteriorly stabilised?: A pulsed fluoroscopic investigation. Bone Jt Res 5:80–86.

19. Koo S, Andriacchi TP. 2008. The knee joint center of rotation is predominantly on the lateral side during normal walking. J Biomech 41:1269–1273.

20. Guan S, Gray HA, Keynejad F, Pandy MG. 2016. Mobile biplane X-ray imaging system for measuring 3D dynamic joint motion during overground gait. Med Imaging, IEEE Trans 35:326–336.

21. Lai A, Lichtwark GA, Schache AG, et al. 2015. In-vivo behavior of the human soleus muscle with increasing walking and running speeds. J Appl Physiol 118:1266–1275.

22. Gray HA, Guan S, Pandy MG. 2017. Accuracy of mobile biplane X-ray imaging in measuring 6-degree-of-freedom patellofemoral kinematics during overground gait. J Biomech 57:152–156.

Author Manuscript

23. Pieper S, Lorensen B, Schroeder W, Kikinis R. 2006. The NA-MIC Kit: ITK, VTK, pipelines, grids and 3D Slicer as an open platform for the medical image computing community. In: 3rd IEEE International Symposium on Biomedical Imaging: Macro to Nano, 2006. Arlington, VA: IEEE; p 698–701.

24. Grood ES, Suntay WJ. 1983. A joint coordinate system for the clinical description of three-dimensional motions: application to the knee. J Biomech Eng 105:136–44.

25. Guan S, Gray HA, Schache AG, et al. 2017. In vivo six-degree-of-freedom knee-joint kinematics in overground and treadmill walking following total knee arthroplasty. J Orthop Res 35:1634–1643.

26. Asano T, Akagi M, Tanaka K, et al. 2001. In vivo three-dimensional knee kinematics using a biplanar image-matching technique. Clin Orthop Relat Res 388:157–166.

27. Krevolin JL, Pandy MG, Pearce JC. 2004. Moment arm of the patellar tendon in the human knee. J Biomech 37:785–8.

28. Yamokoski JD, Banks SA. 2011. Does close proximity robot motion tracking alter gait? Gait Posture 34:508–513.

29. Defrate LE, Sun H, Gill TJ, et al. 2004. In vivo tibiofemoral contact analysis using 3D MRI-based knee models. J Biomech 37:1499–1504.

30. Wilson DR, Feikes JD, Zavatsky AB, O'Connor JJ. 2000. The components of passive knee movement are coupled to flexion angle. J Biomech 33:465–473.

31. Trent PS, Walker PS, Wolf B. 1976. Ligament length patterns, strength, and rotational axes of the knee joint. Clin Orthop Relat Res 117:263–270.

Author Manuscript

32. Sutherland DH. 2001. The evolution of clinical gait analysis part 1: Kinesiological EMG. Gait Posture 14:61–70.

33. Shelburne KB, Pandy MG, Anderson FC, Torry MR. 2004. Pattern of anterior cruciate ligament force in normal walking. J Biomech 37:797–805.

34. Cappellini G, Ivanenko YP, Poppele RE, Lacquaniti F. 2006. Motor Patterns in Human Walking and Running. J Neurophysiol 95:3426–3437.

35. Liu F, Kozanek M, Hosseini A, et al. 2010. In vivo tibiofemoral cartilage deformation during the stance phase of gait. J Biomech 43:658–665.

36. Rainbow MJ, Miranda DL, Cheung RTH, et al. 2013. Automatic determination of an anatomical coordinate system for a three-dimensional model of the human patella. J Biomech 46:2093–6.

Author Manuscript

Table Captions

Table 1: Peak-to-peak displacement (PTPD) of the mean 6-DOF kinematic parameters measured for the tibiofemoral joint (TFJ) and patellofemoral joint (PFJ) for one stride cycle of overground walking.

Table 2: Statistical comparison of 6-DOF kinematic parameters, condylar motion, and locations of the contact centers for the tibiofemoral joint (TFJ) and patellofemoral joint (PFJ) measured for walking and standing.

Figure captions

Figure 1: Schematic diagram illustrating the experimental setup for measuring knee-joint kinematics during overground walking. (A) The Mobile Biplane X-ray (MoBiX) imaging system, comprising two X-ray units and a custom robotic gantry mechanism, enabled horizontal and vertical motion along guides. A high-speed camera (Tracking Camera) acquired images of a retro-reflective marker located on the lateral side of the right knee. These images were processed by a real-time computer (Gantry Motion Profiler) to generate velocity commands controlling the motion of the X-ray units via the servomotors. Two high-speed digital cameras mounted on the two image intensifiers were used to capture biplane X-ray images which were then stored on the Operator Workstation. (B) Plan view of the walkway showing locations of the force plates and approximate foot placement used during each gait trial. Kinematic data were processed for one complete stride cycle, from the 3rd heel-strike to the 4th heel-strike of the right leg (R3 to R4).

Figure 2: Coordinate systems used to define the relative positions and orientations of the femur, tibia and patella of a right knee. (A) The femoral coordinate system was constructed by fitting a cylinder to the posterior and distal portions of both femoral condyles. The axis of the cylinder was defined as the femoral X-axis (X_F) pointing to the right. The origin (O_F) was defined as the foot of the perpendicular dropped from the intercondylar notch apex to the X-axis. A cone was fitted to the femoral diaphysis to determine the long axis (L_1) of the femoral shaft. The Y-axis (Y_F) pointed anteriorly and was mutually perpendicular to X_F and L_1. The Z-axis (Z_F) pointed proximally and was mutually perpendicular to X_F and Y_F. (B) The tibial coordinate system was constructed by fitting a cone to the tibial diaphysis to determine the location of the long axis (L_2) of the tibia. The Z-axis (Z_T) was parallel to L_2 and pointed proximally, passing through the

Author Manuscript

midpoint between the two intercondylar eminences. The relative positions of the femur and tibia, as obtained from the CT scan with the knee unloaded and fully extended, were used to locate the origin (O_T) of the tibial reference frame. The origin (O_T) was located at the foot of the perpendicular dropped from O_F to Z_T. The Y-axis (Y_T) pointed anteriorly and was mutually perpendicular to Z_T and the line (L_3) connecting the approximate center of each tibial plateau. The X-axis (X_T) pointed to the right and was mutually perpendicular to Z_T and Y_T. For the patellar coordinate system, the origin (O_P) was located at the centroid of the patella. The Y-axis (Y_P) pointed anteriorly while the X-axis (X_P) pointed to the right and was mutually perpendicular to Y_P and the posterior patellar ridge. The Z-axis (Z_P) pointed superiorly and was mutually perpendicular to X_P and Y_P [36]. (C) The X_F axis of the femur, Z_T axis of the tibia and Z_P axis of the patella were used as the respective body-fixed axes to define the relative positions and orientations of the bones at the tibiofemoral and patellofemoral joints[24]. Two floating axes (W_T and W_P) that were perpendicular to X_F were defined to also be perpendicular to Z_T and Z_P, respectively. For the tibiofemoral joint, flexion (R_1), abduction (R_2) and external rotation (R_3) were defined by the X_F, W_T and Z_T axes, respectively, while lateral shift (T_1), anterior drawer (T_2) and joint distraction (T_3) were defined along X_F, W_T and Z_T, respectively. For the patellofemoral joint, flexion (R_4), lateral rotation (R_5) and lateral tilt (R_6) were defined by the X_F, W_P and Z_P axes, respectively, while lateral shift (T_4), anterior translation (T_5) and superior translation (T_6) were defined along X_F, W_P and Z_P, respectively. Arrows in the figure indicate the positive direction of each degree of freedom.

Figure 3: Tibiofemoral joint kinematics describing displacements of the tibia with respect to the femur for one cycle of overground walking (red and blue) and standing (green). (A) 6-DOF tibiofemoral kinematics plotted against percentage of the stride cycle; solid and dotted lines

represent mean values calculated for 15 participants and the shaded area represents ±1 standard deviation from the mean. (B) Mean 6-DOF tibiofemoral displacements plotted against the mean knee flexion angle for all 15 participants. The coefficients of determination (r^2) and root mean square error (RMSE) indicating degree of coupling with knee flexion angle are given. RMSE values are in degrees for data given in the top panel and mm for data in the bottom panel. HS, heel-strike; TO, toe-off; CHS, contralateral heel-strike; CTO, contralateral toe-off.

Figure 4: Patellofemoral joint kinematics describing displacements of the patella with respect to the femur for one cycle of overground walking (red and blue) and standing (green). (A) 6-DOF patellofemoral kinematics plotted against percentage of the stride cycle; solid and dotted lines represent mean values calculated for 14 participants and the shaded area represents ±1 standard deviation from the mean. Patellofemoral motion was measured for only 14 participants because the patella moved outside the X-ray image capture volume for one individual. (B) Mean 6-DOF patellofemoral displacements plotted against the mean knee flexion angle for 14 participants. The black dotted line of unit gradient (top left-hand panel) represents the knee flexion angle. The coefficients of determination (r^2) and root mean square error (RMSE) indicating degree of coupling with knee flexion angle are given. RMSE values are in degrees for data given in the top panel and mm for data in the bottom panel. Positive lateral rotation represents the inferior patella moving laterally; positive lateral tilt represents movement of the lateral side of the patella toward the femur. HS, heel-strike; TO, toe-off; CHS, contralateral heel-strike; CTO, contralateral toe-off.

Author Manuscript

Figure 5: Locations of the centers of the femoral condyles for standing and for one complete cycle of overground walking. (A) Locations of the femoral condylar centers projected onto the plateau of the right tibia as viewed from above. The solid red lines represent the stance phase of walking while the dashed blue lines represent the swing phase. The green diamonds represent standing. (B) Locations of the femoral condylar centers plotted against the percentage of the stride cycle. The solid red lines represent the stance phase of walking while the dashed blue lines represent the swing phase. The solid green lines represent standing. The solid and dotted lines represent the mean for 15 subjects, and the shaded area represents ±1 standard deviation from the mean. (C) Locations of the femoral condylar centers plotted against the mean knee flexion angle. The solid red lines represent the stance phase of walking while the dashed blue lines represent the swing phase. The green diamonds represent standing. The coefficients of determination (r^2) and root mean square error (RMSE in mm) indicating degree of coupling with knee flexion angle are indicated in panel (C). HS, heel-strike; CTO, contralateral toe-off; CHS, contralateral heel-strike; TO, toe-off. Results shown in all panels are expressed in the tibial reference frame.

Figure 6: Locations of the tibiofemoral joint contact centers for standing and for one complete cycle of overground walking. (A) Locations of the tibiofemoral contact centers displayed on the right tibia as viewed from above. The solid red lines represent the stance phase of walking while the dashed blue lines represent the swing phase. The green diamonds represent standing. (B) Locations of the tibiofemoral contact centers plotted against the percentage of the stride cycle. The solid red lines represent the stance phase of walking while the dashed blue lines represent the swing phase. The solid green lines represent standing. The solid and dotted lines represent the mean for 15 subjects, and the shaded area represents ±1 standard deviation from the mean.

Author Manuscript

(C) Locations of the tibiofemoral contact centers plotted against the mean knee flexion angle. The solid red lines represent the stance phase of walking while the dashed blue lines represent the swing phase. The green diamonds represent standing. The coefficients of determination (r^2) and root mean square error (RMSE in mm) indicating degree of coupling with knee flexion angle are indicated in panel (C). HS, heel-strike; CTO, contralateral toe-off; CHS, contralateral heel-strike; TO, toe-off.

Figure 7: Locations of the patellofemoral joint contact centers for standing and for one complete cycle of overground walking. (A) Locations of the patellofemoral contact centers displayed on the posterior surface of the right patella as viewed from the posterior direction. The solid red lines represent the stance phase of walking while the dashed blue lines represent the swing phase. The green diamonds represent standing. (B) Locations of the patellofemoral contact centers plotted against the percentage of the stride cycle. The solid red lines represent the stance phase of walking while the dashed blue lines represent the swing phase. The solid green lines represent standing. The solid and dotted lines represent the mean for 14 subjects, and the shaded area represents ±1 standard deviation from the mean. (C) Locations of the patellofemoral contact centers plotted against the mean knee flexion angle. The solid red lines represent the stance phase of walking while the dashed blue lines represent the swing phase. The green diamonds represent standing. The coefficients of determination (r^2) and root mean square error (RMSE in mm) indicating degree of coupling with knee flexion angle are indicated in panel (C). HS, heel-strike; CTO, contralateral toe-off; CHS, contralateral heel-strike; TO, toe-off.

Author Manuscript

Figure 8: Location of the center of rotation of the tibia relative to the femur in the transverse plane measured for one stride cycle of overground walking (top panel); for the stance phase only (middle panel); and for the swing phase only (bottom panel). The blue dots signify the center of rotation calculated for each participant while the larger red dot represents the mean center of rotation calculated for all 15 participants. The red bars represent ±1 standard deviation from the mean.

Figure 9: 6-DOF tibiofemoral joint kinematics measured in the present study (red) compared to results reported by LaFortune et al.[2] (blue) and Andriacchi et al.[3] (green). To ensure a meaningful comparison between the three data sets, the results for all three studies are expressed using the bone coordinate systems described by LaFortune et al.[2] (see also Figs 4 and 5 in Andriacchi et al.[3]). The kinematic profiles for lateral shift, anterior drawer and joint distraction were offset so that the mean value of each trajectory over the stride cycle was zero. The solid and dotted lines represent the mean values for all subjects in each study while the shaded area represents ±1 standard deviation for data recorded in the present study. HS, heel-strike; TO, toe-off; CHS, contralateral heel-strike; CTO, contralateral toe-off.

Author Manuscript

Table 1: Peak-to-peak displacement (PTPD) of the mean 6-DOF kinematic parameters measured for the tibiofemoral joint (TFJ) and patellofemoral joint (PFJ) for one stride cycle of overground walking.

	6-DOF TFJ kinematics		6-DOF PFJ kinematics	
	Parameter	PTPD	Parameter	PTPD
Rotations (deg)	Flexion	70.66	Flexion	50.49
	Abduction	1.94	Lateral Rotation	3.84
	External Rotation	9.23	Lateral Tilt	4.46
Translations (mm)	Lateral Shift	3.96	Lateral Shift	4.92
	Anterior Drawer	6.42	Anterior Translation	11.33
	Joint Distraction	0.97	Superior Translation	14.92

Table 2: Statistical comparison of 6-DOF kinematic parameters, condylar motion, and locations of the contact centers for the tibiofemoral joint (TFJ) and patellofemoral joint (PFJ) measured for walking and standing.

Joint	Parameter (unit)	Dir.	Variable 1				Variable 2				Diff.	95% CI	p-value
			Activity	Con.	Meas.	Value	Activity	Con.	Meas.	Value			
TFJ	Flexion (deg)	-	Stand	-	Mean	-5.81	Walk	-	Mean	21.49	27.30	24.41,30.20	<0.001*
	Abduction (deg)	-	Stand	-	Mean	-4.10	Walk	-	Mean	-4.68	-0.58	-1.30,0.14	0.106
	External rotation (deg)	-	Stand	-	Mean	8.07	Walk	-	Mean	-1.37	-9.44	-11.47,-7.42	<0.001*
	Lateral shift (mm)	-	Stand	-	Mean	2.54	Walk	-	Mean	1.07	-1.46	-2.02,-0.90	<0.001*
	Anterior drawer (mm)	-	Stand	-	Mean	-0.75	Walk	-	Mean	2.58	3.34	2.47,4.20	<0.001*
	Joint distraction (mm)	-	Stand	-	Mean	-0.74	Walk	-	Mean	-1.72	-0.97	-1.57,-0.38	0.004*
PFJ	Flexion (deg)	-	Stand	-	Mean	0.54	Walk	-	Mean	15.72	15.18	13.02,17.34	<0.001*
	Lateral rotation (deg)	-	Stand	-	Mean	-0.86	Walk	-	Mean	-3.06	-2.19	-4.34,-0.05	0.046*
	Lateral tilt (deg)	-	Stand	-	Mean	1.50	Walk	-	Mean	1.71	0.21	-1.04,1.45	0.729
	Lateral shift (mm)	-	Stand	-	Mean	8.62	Walk	-	Mean	4.52	-4.10	-5.42,-2.78	<0.001*
	Anterior translation (mm)	-	Stand	-	Mean	50.10	Walk	-	Mean	46.15	-3.95	-5.28,-2.62	<0.001*
	Superior translation (mm)	-	Stand	-	Mean	9.10	Walk	-	Mean	10.51	1.41	-1.81,4.63	0.362
TFJ	Flexion (deg)	-	Stand	-	Mean	-5.81	Walk	-	Min	-3.23	2.58	0.49,4.67	0.019*
	External rotation (deg)	-	Stand	-	Mean	8.07	Walk	-	Max	5.04	-3.03	-4.79,-1.28	0.002*
TFJ	Condylar center (mm)	AP	Stand	M	Mean	-3.24	Stand	L	Mean	3.44	6.68	4.45,8.91	<0.001*
		AP	Stand	L	Mean	3.44	Walk	L	Max	2.04	1.4	0.44,2.36	0.007*
		AP	Walk	M	PTPD	7.62	Walk	L	PTPD	11.57	3.95	2.16,5.73	<0.001*
		ML	Walk	M	PTPD	6.21	Walk	L	PTPD	6.23	0.02	-0.28,0.32	0.878
		SI	Walk	M	PTPD	3.62	Walk	L	PTPD	3.45	0.18	-0.83,0.47	0.569
TFJ	Contact center (mm)	AP	Stand	M	Mean	3.15	Stand	L	Mean	9.32	6.17	2.27,10.07	0.004*
		AP	Stand	L	Mean	9.32	Walk	L	Max	6.19	-3.13	0.12,6.15	0.042*
		AP	Walk	M	PTPD	9.69	Walk	L	PTPD	15.38	5.69	2.47,8.91	0.002*
		ML	Walk	M	PTPD	6.87	Walk	L	PTPD	7.67	0.81	-0.96,2.59	0.344
PFJ	Contact center (mm)	ML	Stand	L	Mean	5.96	Walk	L	Mean	12.08	-6.12	-9.49,-2.75	0.002*
		ML	Walk	M	PTPD	13.21	Walk	L	PTPD	16.21	3	-0.32,6.33	0.074
		SI	Walk	M	PTPD	21.5	Walk	L	PTPD	20.76	-0.73	-2.41,0.95	0.363

*Indicates a significant difference ($p<0.05$)

Column headers: Dir. – Direction, Diff. – Difference, Con. – Condyle, Meas. – Measurement, CI – Confidence Interval;

Direction column: AP – Anterior-Posterior, ML – Medial-Lateral and SI – Superior-Inferior;

Condyle column: M – Medial, L – Lateral;

Measurement column: Min, Max, Mean and PTPD are the Minimum, Maximum, Mean and Peak-To-Peak Displacements measured over the activity for each participant and averaged across all participants.

Author Manuscript

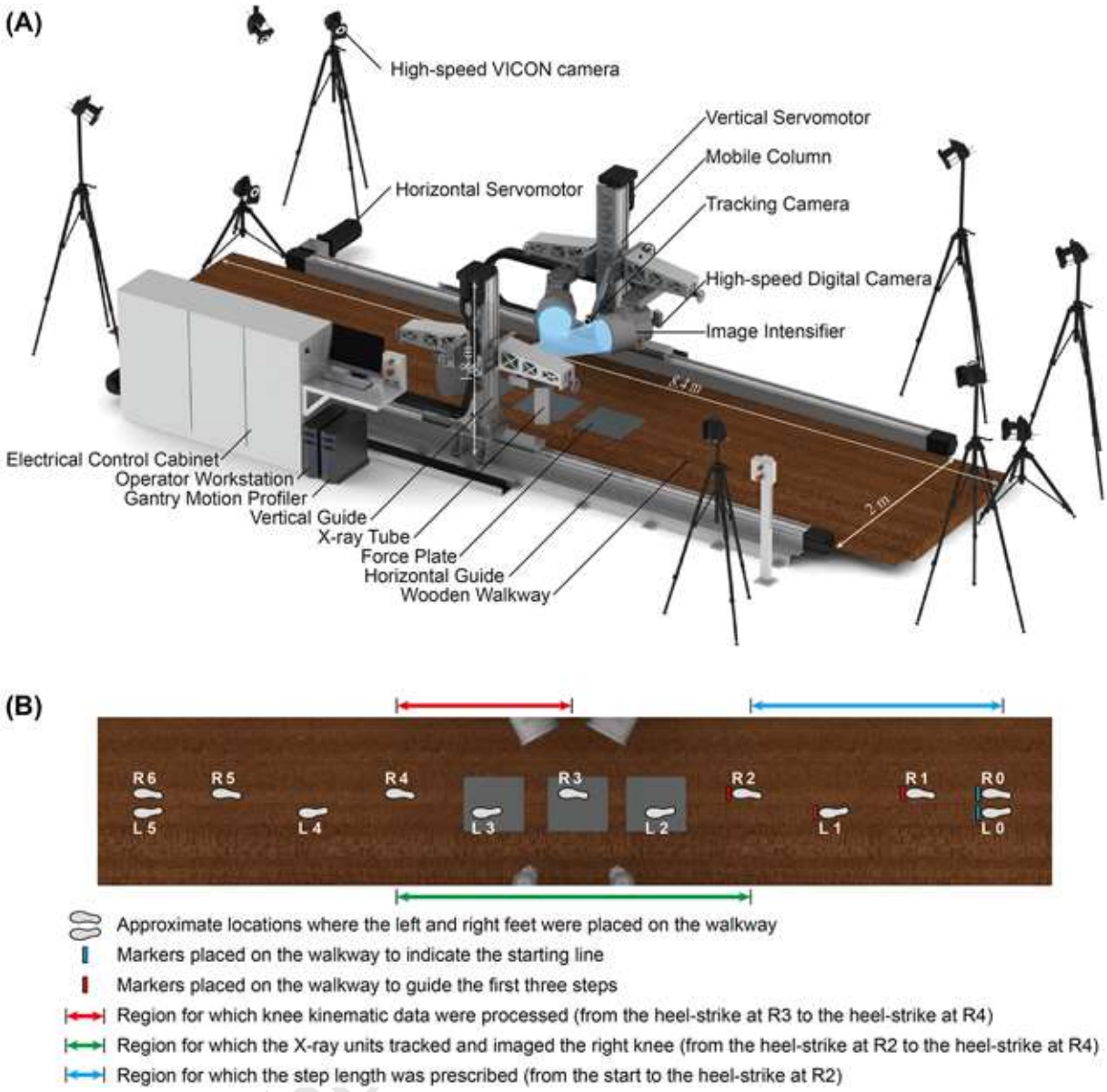

Figure 1

Author

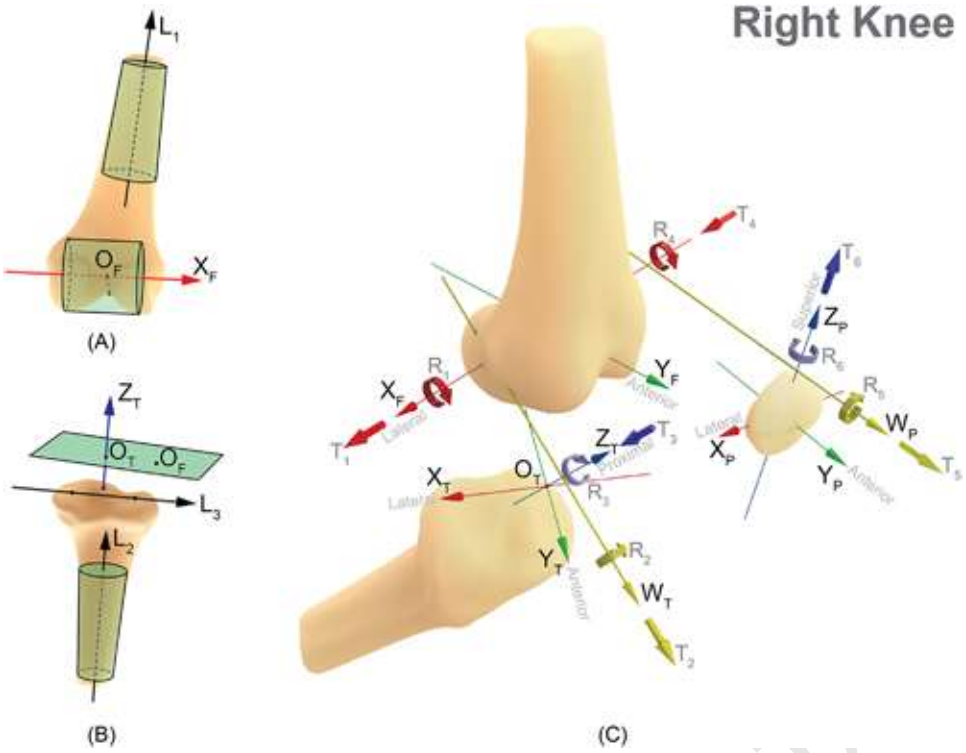

Figure 2

Author Manuscript

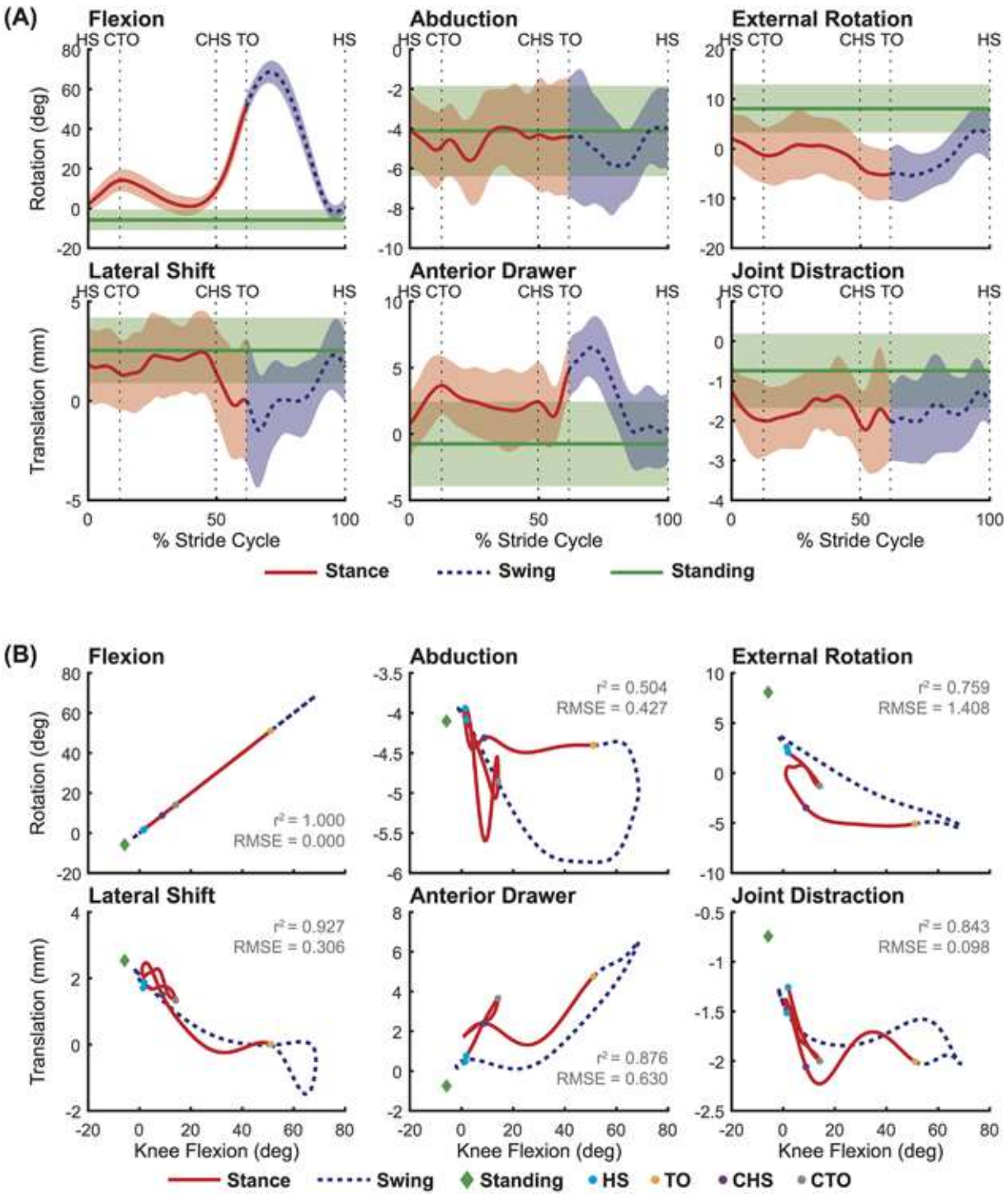
(A)
Flexion
Abduction
External Rotation
Lateral Shift
Anterior Drawer
Joint Distraction
HS CTO
CHS TO
HS
Rotation (deg)
Translation (mm)
% Stride Cycle
Stance
Swing
Standing
(B)
r² = 1.000
RMSE = 0.000
r² = 0.504
RMSE = 0.427
r² = 0.759
RMSE = 1.408
r² = 0.927
RMSE = 0.306
r² = 0.876
RMSE = 0.630
r² = 0.843
RMSE = 0.098
Knee Flexion (deg)
Stance
Swing
Standing
HS
TO
CHS
CTO

Figure 3

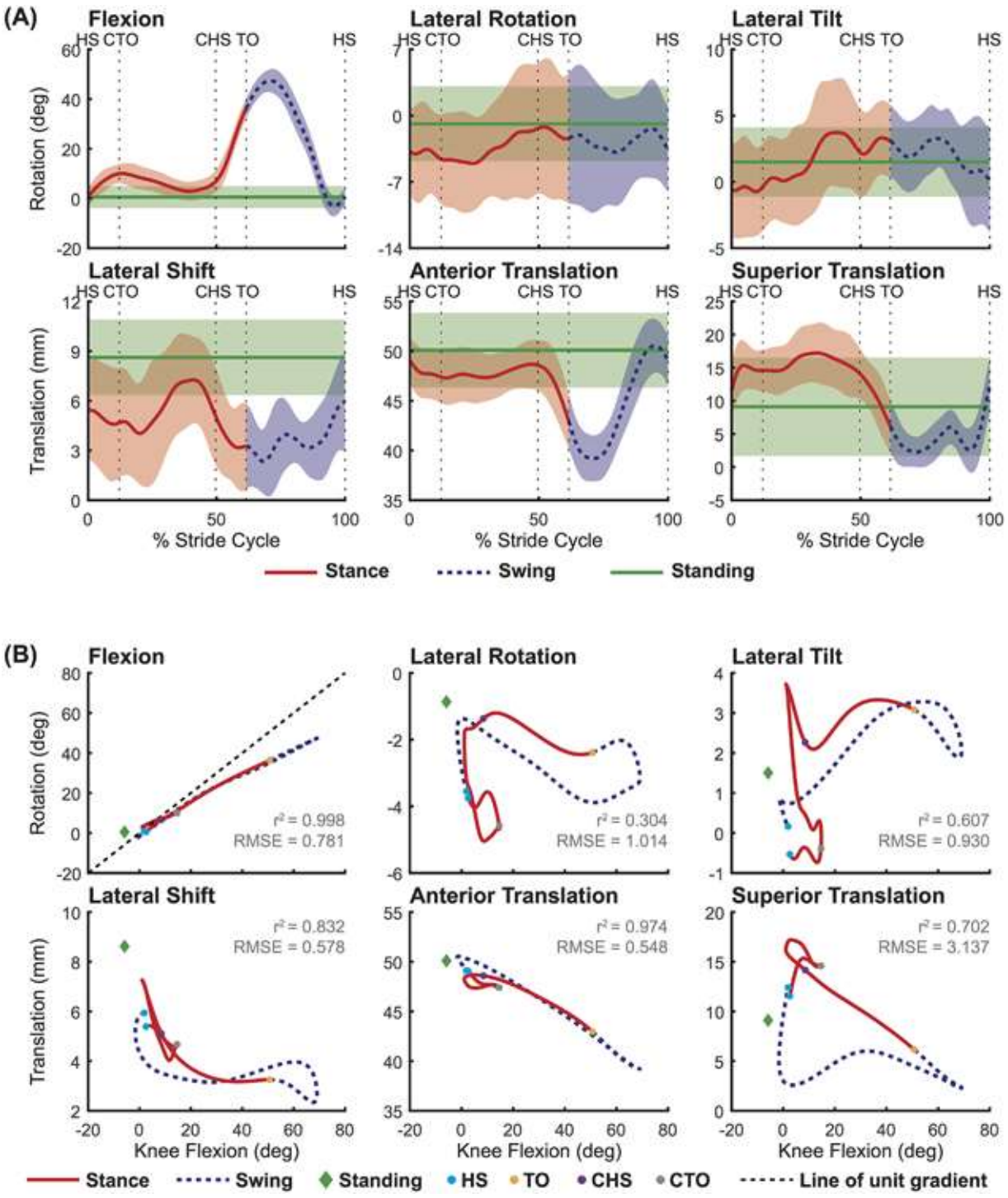
(A)
Flexion
Lateral Rotation
Lateral Tilt
Lateral Shift
Anterior Translation
Superior Translation
HS CTO
CHS TO
HS
Rotation (deg)
Translation (mm)
% Stride Cycle
Stance
Swing
Standing
(B)
Flexion
Lateral Rotation
Lateral Tilt
Lateral Shift
Anterior Translation
Superior Translation
r² = 0.998
RMSE = 0.781
r² = 0.304
RMSE = 1.014
r² = 0.607
RMSE = 0.930
r² = 0.832
RMSE = 0.578
r² = 0.974
RMSE = 0.548
r² = 0.702
RMSE = 3.137
Knee Flexion (deg)
Stance
Swing
Standing
HS
TO
CHS
CTO
Line of unit gradient

Figure 4

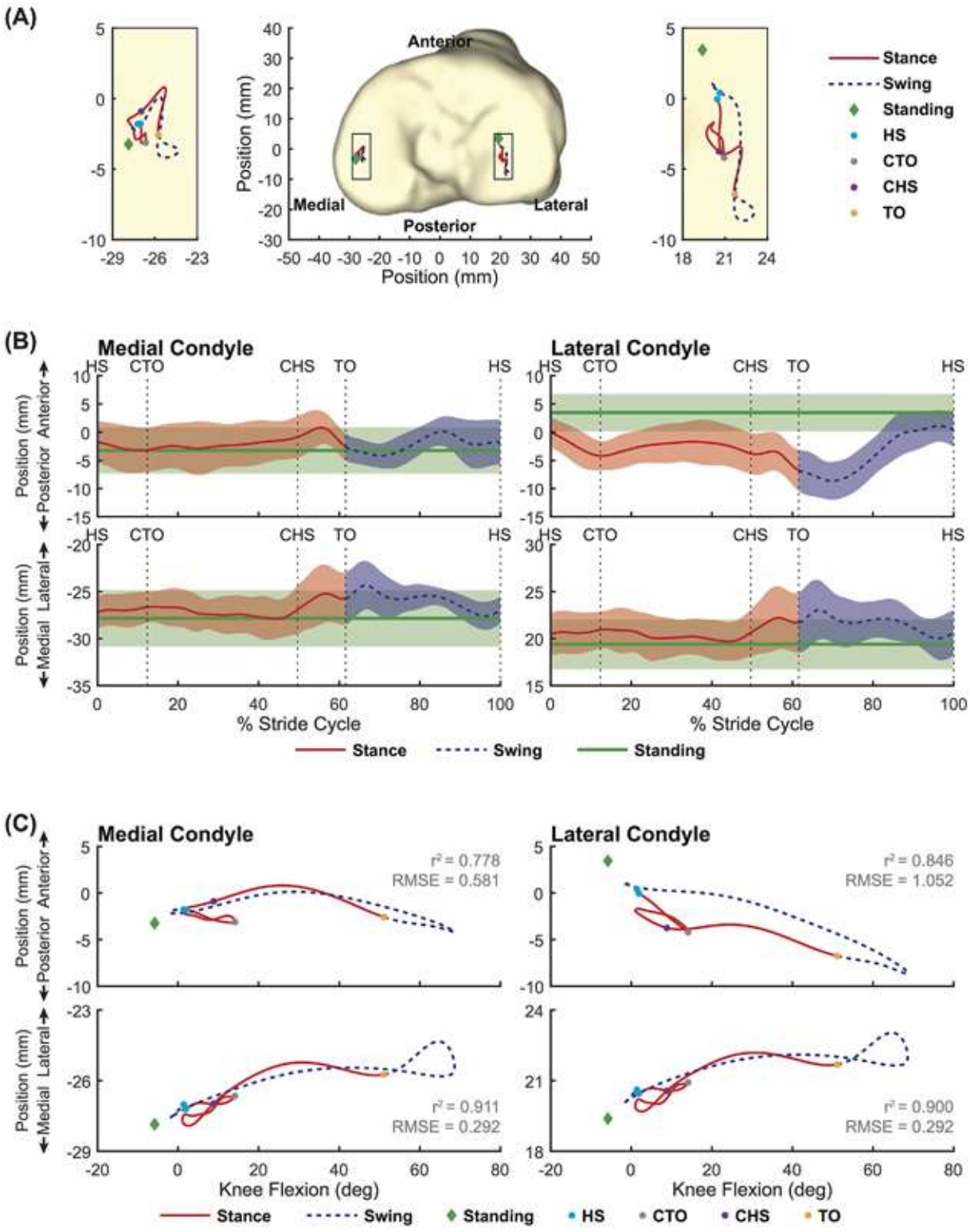
(A)
Anterior
Medial
Lateral
Posterior
Position (mm)
Position (mm)
Stance
Swing
Standing
HS
CTO
CHS
TO
(B)
Medial Condyle
Lateral Condyle
HS
CTO
CHS
TO
Position (mm) Posterior Anterior
Position (mm) Medial Lateral
% Stride Cycle
Stance
Swing
Standing
(C)
Medial Condyle
Lateral Condyle
r² = 0.778
RMSE = 0.581
r² = 0.846
RMSE = 1.052
r² = 0.911
RMSE = 0.292
r² = 0.900
RMSE = 0.292
Position (mm) Posterior Anterior
Position (mm) Medial Lateral
Knee Flexion (deg)
Stance
Swing
Standing
HS
CTO
CHS
TO

Figure 5

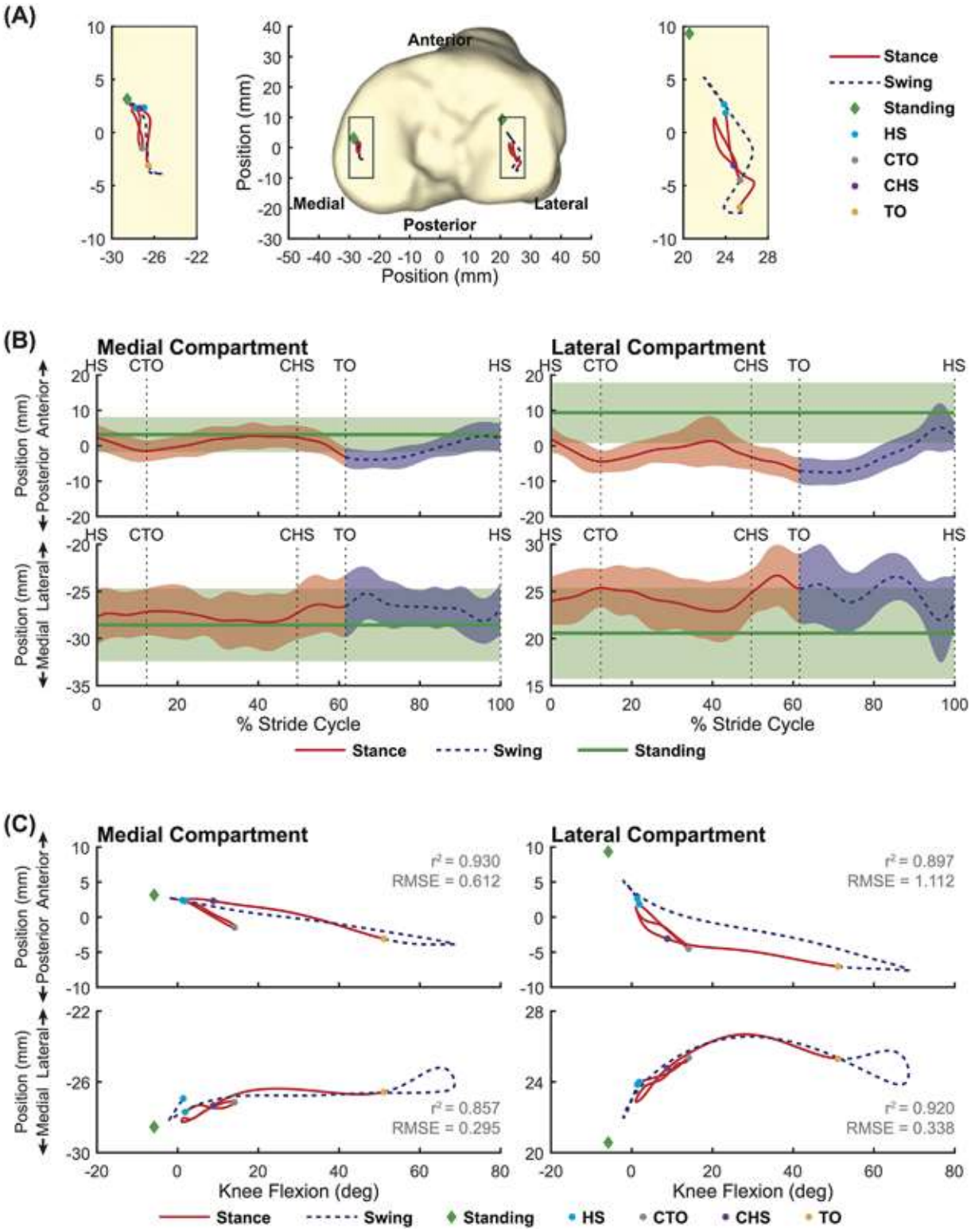
(A)
Anterior
Medial
Lateral
Posterior
Position (mm)
Position (mm)
Stance
Swing
Standing
HS
CTO
CHS
TO
(B)
Medial Compartment
Lateral Compartment
Position (mm) Posterior Anterior
Position (mm) Medial Lateral
% Stride Cycle
% Stride Cycle
Stance
Swing
Standing
(C)
Medial Compartment
Lateral Compartment
r² = 0.930
RMSE = 0.612
r² = 0.897
RMSE = 1.112
r² = 0.857
RMSE = 0.295
r² = 0.920
RMSE = 0.338
Position (mm) Posterior Anterior
Position (mm) Medial Lateral
Knee Flexion (deg)
Knee Flexion (deg)
Stance
Swing
Standing
HS
CTO
CHS
TO

Figure 6

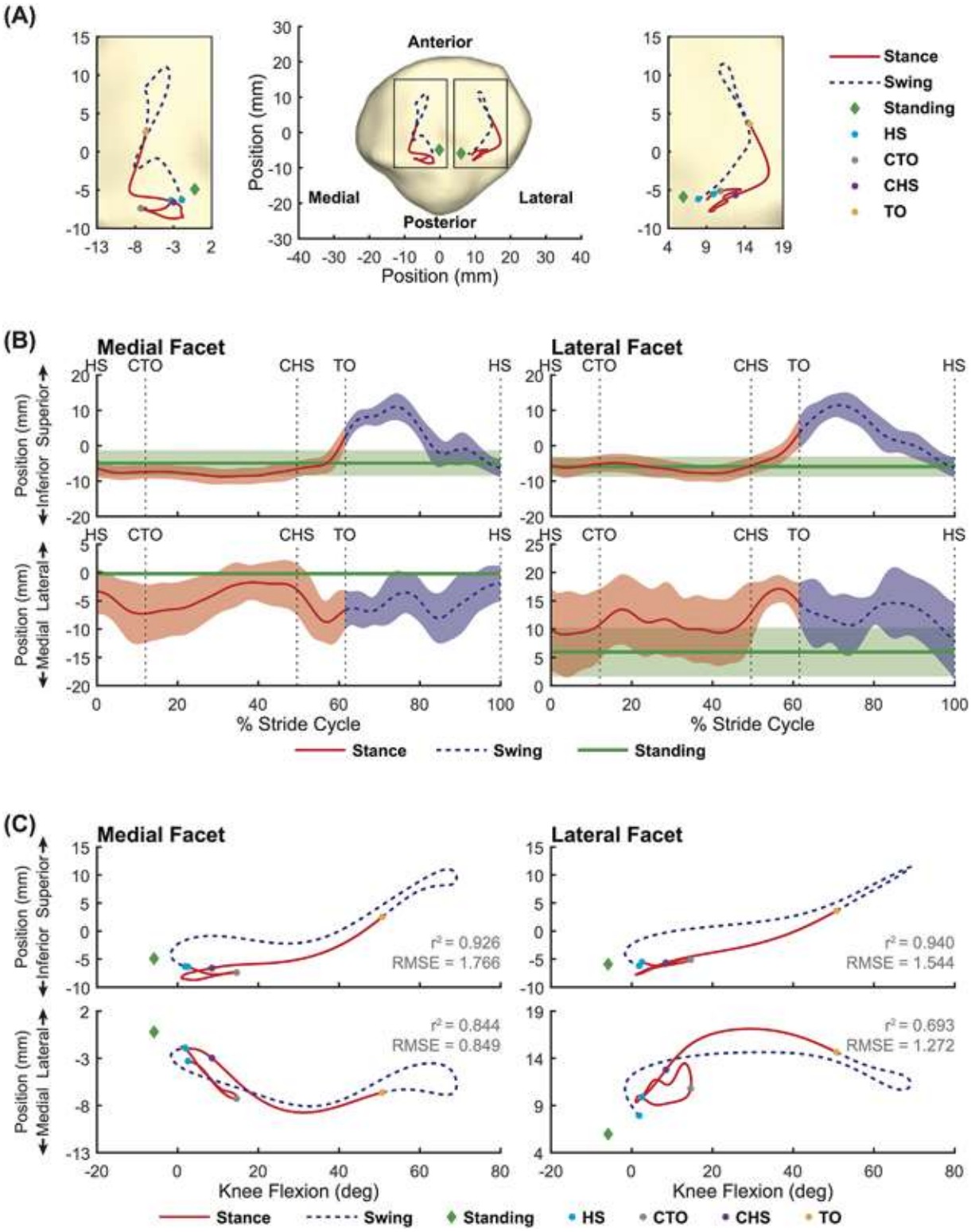
(A)
Anterior
Medial
Lateral
Posterior
Position (mm)
Position (mm)
Stance
Swing
Standing
HS
CTO
CHS
TO
(B)
Medial Facet
Lateral Facet
HS
CTO
CHS
TO
HS
Position (mm)
Inferior Superior
Position (mm)
Medial Lateral
% Stride Cycle
% Stride Cycle
Stance
Swing
Standing
(C)
Medial Facet
Lateral Facet
Position (mm)
Inferior Superior
Position (mm)
Medial Lateral
r² = 0.926
RMSE = 1.766
r² = 0.940
RMSE = 1.544
r² = 0.844
RMSE = 0.849
r² = 0.693
RMSE = 1.272
Knee Flexion (deg)
Knee Flexion (deg)
Stance
Swing
Standing
HS
CTO
CHS
TO

Figure 7

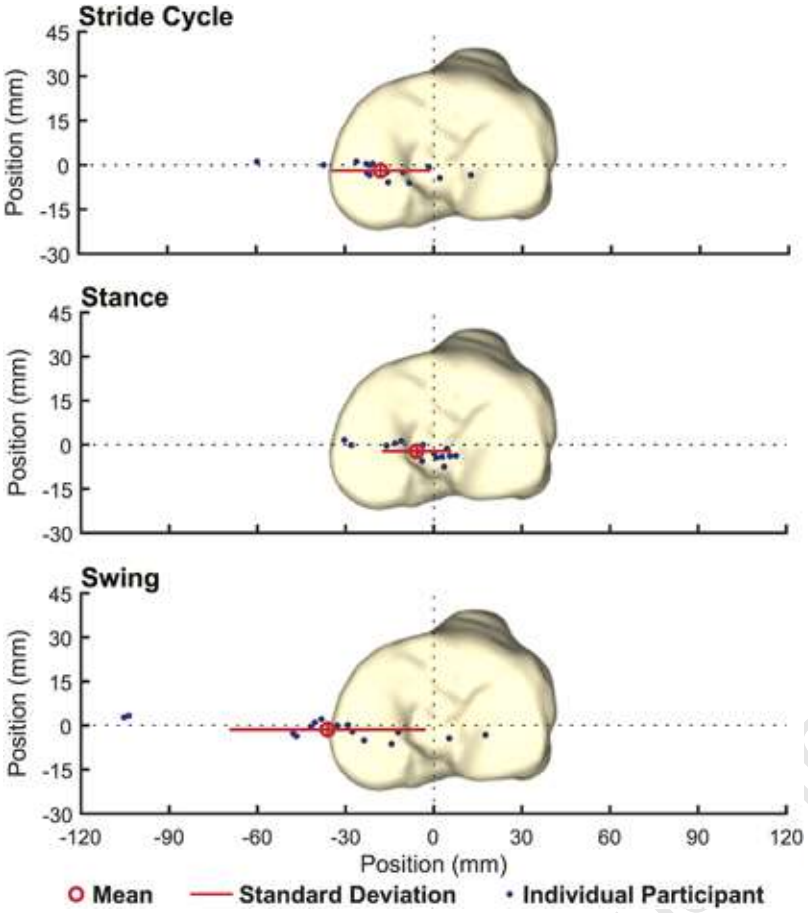

Figure 8

Author Manuscript

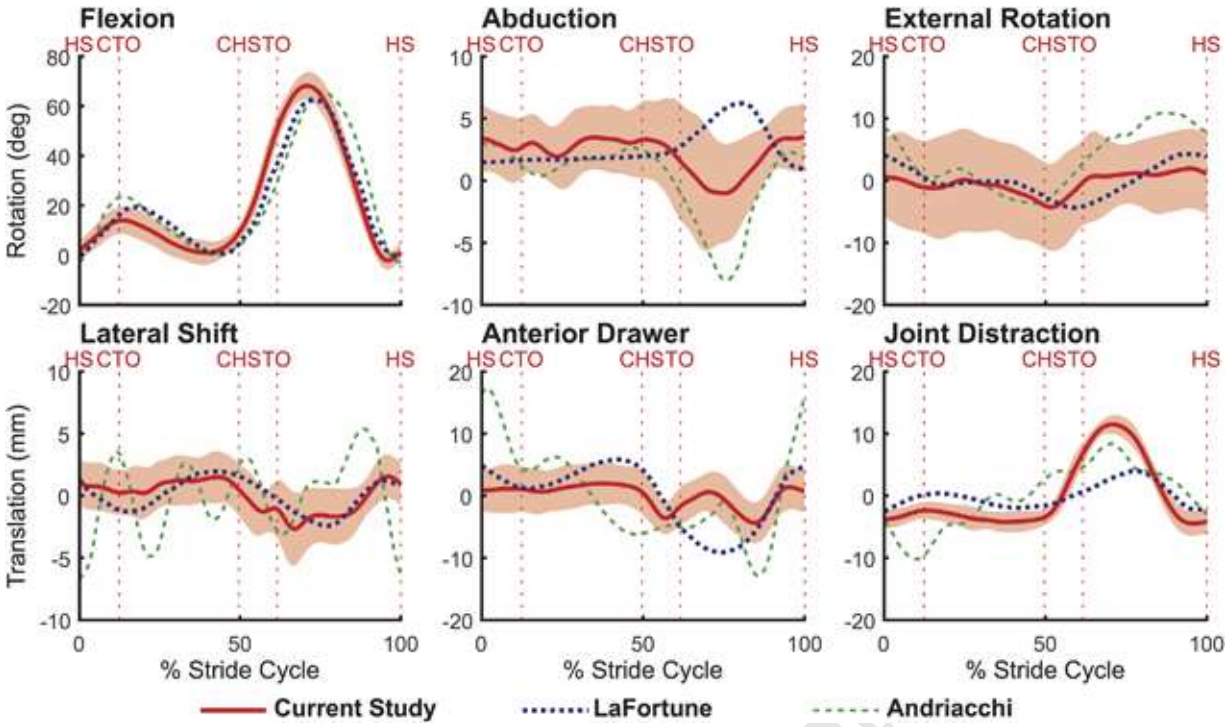

Figure 9

Author Manuscript